

Optimal condition-based maintenance decision-making for nonlinear degrading systems: A time-scale transformed wiener process modeling approach

Bo Zhu^{a†}, Enzhi Dong^{a†}, Zhonghua Cheng^{a*}, Kexin Jiang^a and Shuai Yue^a

^aShijiazhuang Campus of Army Engineering University of PLA, China

[†]These authors contributed equally to this work.

CHRONICLE

Article history:

Received October 25 2025

Received in Revised Format

January 28 2026

Accepted March 5 2026

Available online March 5
2026

Keywords:

Wiener process

Time-scale transformation

Nonlinear degradation

Condition-Based Maintenance

ABSTRACT

Effective strategies for Prognostics and Health Management (PHM) are fundamental to advancing the operational integrity and economic sustainability of complex industrial assets. Overcoming the persistent hurdle of modeling the intricate temporal nonlinearities and stochastic behaviors inherent in degradation processes is central to this endeavor. This study introduces an optimized maintenance framework based on real-time condition monitoring for systems subject to stochastic wear, utilizing an innovative nonlinear Wiener process model with time-scale transformation. By framing the optimization objective as the minimization of the long-term average cost rate, we derive explicit expressions for the optimal inspection interval and the threshold for preventive maintenance. A likelihood ratio test demonstrates the superiority of the nonlinear model over linear alternatives. A case study on a Power Take-Off (PTO) unit validates the effectiveness of the proposed method, showing its ability to balance failure risk and maintenance cost efficiently. The proposed strategy provides a practical and scientifically grounded tool for managing systems with nonlinear degradation characteristics.

© 2026 by the authors; licensee Growing Science, Canada

1. Introduction

In critical sectors like aerospace and energy, system reliability fundamentally depends on high-performance equipment (Civera et al., 2022; Sharma, et al., 2021; Lin et al., 2025). Research has shown that system performance tends to deteriorate nonlinearly with service time, which can lead to failures and pose significant risks to operational safety and economic efficiency. Although maintenance is essential to mitigate failure risks associated with degrading systems, maintenance actions often incur considerable costs. For example, maintenance expenses for ball screw components can account for 15% to 70% of their life-cycle costs (Zhang et al., 2022), underscoring the need for optimized maintenance decision-making.

For highly reliable equipment, time-to-failure data are often scarce due to long operational lifetimes. A viable alternative is to construct models using performance degradation data (Gong et al., 2020; Zhu et al., 2026). Equipment degradation refers to the gradual decline in performance parameters over time or under accumulated operational load. This process not only affects the reliability of individual components but may also propagate to multiple components or even endanger the entire system. Accurate modeling of degradation is essential for precise failure prediction and for establishing effective CBM strategies. The ability to forecast system failures and prompt user intervention hinges on the ongoing surveillance and assessment of pivotal parameter degradation, thereby reducing the risk of unexpected breakdowns.

Nonlinearity is a critical factor that must be considered when modeling the degradation processes of complex equipment systems. In recent years, significant attention has been devoted to addressing nonlinearities in stochastic degradation modeling. Many industrial assets exhibit distinct nonlinear degradation patterns, such as slow initial degradation, stable mid-term behavior, and rapid acceleration toward the end of life. Although the classical linear Wiener process is widely used due to its mathematical tractability, its assumption of constant degradation rates often fails to capture realistic nonlinear behavior (Cao et al., 2025; Dong et al., 2024). Despite considerable progress in nonlinear stochastic process-based degradation modeling,

* Corresponding author

E-mail lgdsjzxq@sina.com (Z. Cheng)

ISSN 1923-2934 (Online) - ISSN 1923-2926 (Print)

2026 Growing Science Ltd.

doi: 10.5267/j.ijiec.2026.3.003

effectively integrating the high-quality prognostic information generated by these models into maintenance decision frameworks remains a challenge. Most existing CBM strategies either rely on simplified linear models or fail to fully account for the nonlinear dynamics of degradation processes in their decision mechanisms.

To address these limitations, recent studies have explored CBM strategies utilizing the nonlinear Wiener process. By incorporating sensor technology for continuous monitoring and introducing a time-scale transformation technique, where physical time is mapped via a power function, the standard Wiener process is converted into a nonlinear degradation path. Maintenance actions are then triggered based on real-time condition monitoring results. This approach preserves the advantages of stochastic process modeling while improving its adaptability to complex degradation patterns. Given this reliance, a detailed examination of equipment performance degradation is vital to guarantee the safe and stable operation (Oh et al., 2024). Furthermore, research on CBM strategies helps facilitate adequate preparation for fault prevention and minimizes losses due to unplanned maintenance.

2. Literature Review

The widespread adoption of Time-Based Maintenance (TBM), driven by its implementation ease rather than efficacy, relies on static schedules derived from historical failures, a methodology misaligned with modern industrial complexity (Alaswad et al., 2017; de Jonge et al., 2017). However, TBM does not account for the actual health conditions of individual equipment, often leading to either over-maintenance or under-maintenance, thereby increasing maintenance costs or failure risks. Shifting from calendar-driven to condition-driven paradigms, CBM leverages real-time monitoring to actuate maintenance, achieving superior cost-risk trade-offs. “Foundational research by Wijnmalen established heuristic control limits for multi-component CBM (Wijnmalen et al., 1997), which Chen et al. later refined into a two-phase opportunistic maintenance model for cost minimization” (Chen et al., 2022). “Xie et al. optimized concurrent maintenance time windows by leveraging the probability distribution of Remaining Useful Life (RUL) and maintenance duration, introducing a comprehensive efficiency metric that incorporates cost rate, reliability, and availability” (Xie et al., 2024). “Liu et al. addressed CBM for batch production systems under fluctuating demand, modeling degradation via a Gamma process with acceleration and improvement factors” (Liu et al., 2025). Equipment health assessment is a critical component of PHM. It typically involves constructing a Health Indicator (HI) curve that exhibits a monotonic trend, where threshold-based evaluation is employed to determine health status (Zhan et al., 2023). Identifying the degradation trend is essential for CBM decision-making, as it enables accurate assessment of the current health state and optimal timing for maintenance interventions. “Under data-limited scenarios, data-driven approach, which leverages penalized logistic regression to model failure probability as a function of degradation for flexible CBM threshold selection, represents a significant methodological advance” (Cai et al., 2025). Prevailing cost analyses within bounded horizons are fundamentally limited: they either default to conventional TBM or engage in methodological compromise by abstracting equipment or multi-component systems into oversimplified constructs, prioritizing computational convenience over model fidelity and practical relevance (Luo et al., 2025; Qiu, et al., 2019; Tan et al., 2025). However, these studies generally overlook the nonlinear characteristics of equipment degradation trends. A prevalent tactic to handle nonlinear degradation is its transformation into an approximate linear domain, thereby enabling established linear models. Illustratively, “Ye et al. separated the workflow into distinct offline and online stages, leveraging historical data for initial parameter estimation to bootstrap subsequent real-time forecasting” (Ye et al., 2015). The random-effects regression model (Lu et al., 1993), pioneered by Lu and Meeker et al., captures common degradation behaviors across populations but fails to adequately account for temporal uncertainties inherent in the degradation process.

In contrast, stochastic processes offer greater flexibility and capability in modeling time-dependent uncertainties, making them particularly suitable for CBM. Gamma processes (Nguyen et al., 2015), inverse Gaussian processes (Li et al., 2022), and Wiener processes (Hao et al., 2025) are among the most widely used stochastic models. Unlike Gamma or IG processes, the Wiener process, with its non-monotonic nature, is well-suited for describing multidirectional variations in degradation levels over time. Consequently, Wiener-based models have been extensively applied in CBM decision-making for various systems and components. For mission-oriented systems subject to dynamic degradation processes, the risk of early failure is often high. For example, Li developed a dynamic CBM optimization model based on the inverse Gaussian degradation process (Li et al., 2022). “Recent advances integrate CBM with operational decision-making. Hao et al. coupled dynamic load allocation via a Markov decision framework” (Hao et al., 2025). Conversely, “Zhang et al. formulated the optimal CBM strategy itself as a continuous-state Markov decision process, minimizing the expected infinite-horizon cost within a diffusion process model” (Zhang et al., 2024).

Despite these advances, current research exhibits several limitations:

- (1) Many studies still rely on linear degradation assumptions or time-based maintenance policies for simplicity, failing to leverage the accurate information provided by nonlinear degradation models.
- (2) Limited attention has been paid to maintenance decision-making over finite time horizons, despite the fact that real-world engineering operations often involve finite planning periods.
- (3) There is insufficient in-depth analysis on parameter estimation and hypothesis testing for key parameters in maintenance models.

3. Nonlinear Wiener Degradation

This section integrates the aforementioned nonlinear degradation model with maintenance decision objectives, aiming to establish a comprehensive mathematical programming framework. The focus is on elucidating the transformation of degradation state information into optimal inspection and maintenance actions.

3.1 Implementation Procedure

To achieve more accurate CBM, the modeling process begins with the degradation characteristics of the equipment. We transcend the limitation of the standard linear Wiener process by introducing a power-function time rescaling. Informed by empirical degradation patterns, we posit that the equipment state evolves according to this nonlinear Wiener process. A specific power-law time transformation is derived, thereby establishing a unified model that captures both the deterministic degradation trajectory and intrinsic stochastic variability. Subsequently, from the perspective of balancing failure risk and maintenance cost, a CBM threshold is derived based on reliability requirements. In practical applications, this involves determining the time-transformation parameters, setting the target reliability level, calculating the maintenance threshold, and iterating over inspection intervals. A mean maintenance cost rate function is then established to support maintenance decision-making. The detailed flowchart of the modeling process is presented to Fig.1.

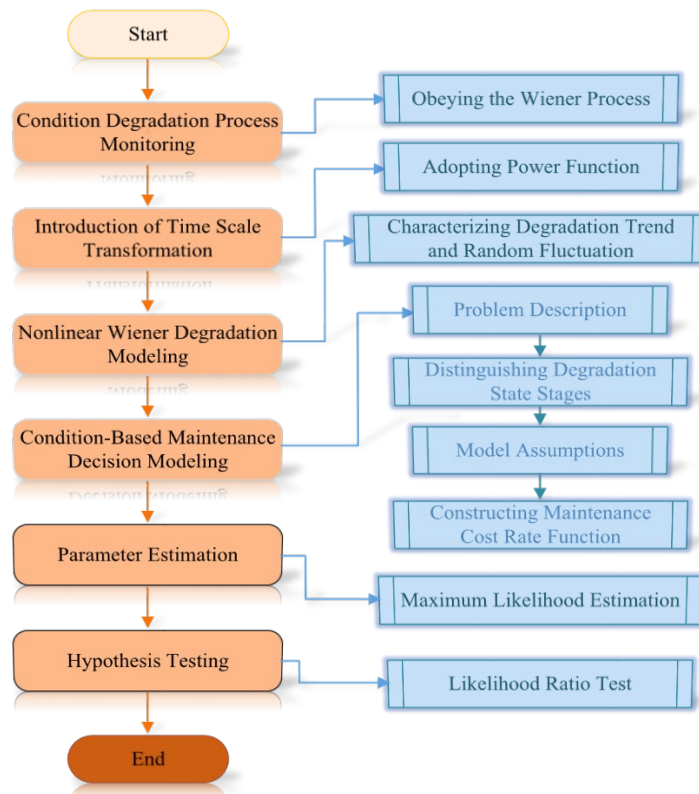


Fig. 1. Workflow Diagram for Constructing the CBM Model

3.2 Nonlinear Wiener Degradation Process

Wiener process fundamentally assumes independent, stationary increments, a mathematical abstraction that may oversimplify complex degradation dynamics. This section models equipment degradation state $X(t)$ through a linear Wiener process defined as:

$$X(t) = x_0 + \lambda t + \sigma B \quad (1)$$

where x_0 is the initial degradation level, λ is the drift coefficient, σ is the diffusion coefficient, and $B(t)$ represents standard Brownian motion capturing random fluctuations, with $B(t) \sim N(0, \sigma^2 t)$. In practice, degradation rates often vary over the equipment's lifetime due to factors such as mechanical wear and operational conditions. Assuming a constant drift in a linear Wiener process may lead to significant underestimation of failure risks in later stages. To address this, we introduce a nonlinear time-scale transformation function $\psi(t)$, which maps real time t to a scaled time $\xi = \psi(t)$. Since practical focus lies on the actual degradation in real time rather than scaled time, and given that $\psi(t)$ is monotonically increasing. Adopting a time-

warping transformation of the Wiener process (Si et al., 2022; Zheng et al., 2024), we arrive at a more general representation of the physical-time degradation trajectory:

$$\tilde{X}(t) = x_0 + \lambda \psi(t) + \sigma B(\psi(t)) \quad (2)$$

Using the properties of independent increments and normality of Brownian motion, the increment of degradation over a future period s from time t_i satisfies:

$$\tilde{X}(t_{i+s}) - \tilde{X}(t_i) \sim N(\lambda \Delta \psi_{i+s}, \sigma^2 \Delta \psi_{i+s}) \quad (3)$$

where $\Delta \psi_{i+s} = \psi(t_{i+s}) - \psi(t_i)$ denotes the increment in scaled time. Assuming the current degradation at time t_i is X_i , the degradation at a future time $t_i + s$ can be expressed as:

$$\tilde{X}(t_{i+s}) - \tilde{X}(t_i) = \lambda[\psi(t_{i+s}) - \psi(t_i)] + \sigma[B(\psi(t_{i+s})) - B(\psi(t_i))] \quad (4)$$

Since mechanical wear, fatigue crack propagation, and other processes in equipment often follow a power-law pattern, the time-scale transformation function is assumed to take the form $\gamma(t) = qt^p$ ($q, p > 0$), where q is an undetermined coefficient and p is the power-law exponent used to together quantify the nonlinear acceleration in degradation evolution. Consequently, the nonlinear Wiener process takes the following compact form:

$$X_n(t_{n,j}) = \tilde{\lambda} \cdot \gamma(t_{n,j}) + \tilde{\sigma} \cdot B(t_{n,j}) \quad (5)$$

where the drift parameter $\tilde{\lambda}$ and diffusion coefficient $\tilde{\sigma}$ require estimation from observed degradation paths. Based on the above research, we use $x_{j,1:M_j} = (x_{j,1}, x_{j,2}, \dots, x_{j,M_j})^T$ to represent the original degradation values of the j -th system.

Furthermore, the mean of the original degradation values of all subsystems can be expressed as $x_{1,N} = x_{1,1:M_1}, x_{2,1:M_2}, \dots, x_{N,M_N}$.

Consequently, monitoring sequence of j -th piece of equipment is:

$$\tilde{X}_j(t) = x_j + \tilde{\lambda} qt_{k_j}^p + \tilde{\sigma} B(qt_{k_j}^p) \quad (6)$$

This section derives a theoretical foundation for subsequent parameter estimation and maintenance decision-making. The next section will focus on discussing the parameter estimation methods and statistical tests of this model, providing support for model identification in practical engineering applications.

4. Estimation and Testing

4.1 Estimation

Accurate parameter estimation is fundamental to the nonlinear Wiener degradation model in Eq. (5). We present a concise maximum likelihood estimation, derived from observed degradation trajectories and building upon the work of Si et al. (Si et al., 2012), to determine these critical parameters.

We define a set of N sampled degradation paths. Each path n is empirically characterized by inspection instants $t_{n,1}, t_{n,2}, \dots, t_{n,m_n}$, with m_n quantifying the inspection count before its failure time. The corresponding degradation magnitude at $t_{n,j}$ is:

$$X_n(t_{n,j}) = \tilde{\lambda} \cdot \gamma(t_{n,j}) + \tilde{\sigma} \cdot B(t_{n,j}) \quad (7)$$

To derive the maximum likelihood estimates for parameters $\tilde{\lambda}$ and $\tilde{\sigma}$, it is essential to formulate the joint probability density function of parameters. According to the theory of multivariate normal distribution, \mathbf{X}_n obeys a multivariate normal distribution with mean $\tilde{\mu}_n$ and variance Σ_n , where:

$$\tilde{\mu}_n = \tilde{\lambda} \mathbf{V}_n, \Sigma_n = \tilde{\sigma}^2 \mathbf{\Omega}_n \quad (8)$$

$$\mathbf{\Omega}_n = \begin{pmatrix} t_{n,1} & t_{n,1} & \cdots & t_{n,1} \\ t_{n,1} & t_{n,2} & \cdots & t_{n,2} \\ \vdots & \vdots & \ddots & \vdots \\ t_{n,1} & t_{n,2} & \cdots & t_{n,m_n} \end{pmatrix} \quad (9)$$

This derivation fundamentally presumes the mutual independence of measurements across degradation trajectories. Under this critical assumption, the joint probability density for the parameter vector $\mathbf{\Lambda} = (\tilde{\lambda}, \tilde{\sigma}^2)^T$ is:

$$P(\mathbf{\Lambda}|\mathbf{X}_n) = -\frac{1}{\sqrt{m_n} \sqrt{2\pi}} |\mathbf{\Sigma}_n|^{-\frac{1}{2}} \exp\left(-\frac{1}{2}(\mathbf{X}_n - \tilde{\lambda}\mathbf{V}_n)' \mathbf{\Sigma}_n^{-1} (\mathbf{X}_n - \tilde{\lambda}\mathbf{V}_n)\right) \quad (10)$$

The consequent log-likelihood function, obtained via a natural logarithmic transformation of Eq. (10), is:

$$\ln P(\mathbf{\Lambda}|\mathbf{X}_n) = -\frac{m_n}{2} (\ln(2\pi) + \ln|\mathbf{\Sigma}_n| + (\mathbf{X}_n - \tilde{\lambda}\mathbf{V}_n)' \mathbf{\Sigma}_n^{-1} (\mathbf{X}_n - \tilde{\lambda}\mathbf{V}_n)) \quad (11)$$

Maximizing this likelihood requires solving for the stationary points. The first-order partial derivatives of Eq. (11) are:

$$\frac{\partial \ln P(\mathbf{\Lambda}|\mathbf{X}_n)}{\partial \tilde{\lambda}} = \mathbf{V}_n' \mathbf{\Sigma}_n^{-1} \mathbf{X}_n - \tilde{\lambda} \mathbf{V}_n' \mathbf{\Sigma}_n^{-1} \mathbf{V}_n \quad (12)$$

$$\frac{\partial \ln P(\mathbf{\Lambda}|\mathbf{X}_n)}{\partial \tilde{\sigma}^2} = -\frac{N}{2\tilde{\sigma}^2} + \frac{1}{2\tilde{\sigma}^4} (\mathbf{X}_n - \tilde{\lambda}\mathbf{V}_n)' \mathbf{\Omega}^{-1} (\mathbf{X}_n - \tilde{\lambda}\mathbf{V}_n) \quad (13)$$

The maximization of this function yields the closed-form maximum likelihood estimates. Setting Eq. (12) and Eq. (13) to zero, equations are:

$$\tilde{\lambda} = \frac{\mathbf{V}_n' \mathbf{\Sigma}_n^{-1} \mathbf{X}_n}{\mathbf{V}_n' \mathbf{\Sigma}_n^{-1} \mathbf{V}_n} = \frac{\mathbf{V}_n' \mathbf{\Omega}^{-1} \mathbf{X}_n}{\mathbf{V}_n' \mathbf{\Omega}^{-1} \mathbf{V}_n} \quad (14)$$

$$\tilde{\sigma}^2 = \frac{1}{N} ((\mathbf{X}_n - \tilde{\lambda}\mathbf{V}_n)' \mathbf{\Omega}^{-1} (\mathbf{X}_n - \tilde{\lambda}\mathbf{V}_n)) \quad (15)$$

4.2 Testing

To statistically justify the necessity of introducing the time-scale transformation, to validate whether the nonlinear model significantly outperforms the standard linear Wiener process model, this section employs the Likelihood Ratio Test (LRT) for model comparison (Bai et al., 2024). Methodologically, the procedure is bifurcated:

Step 1: Hypothesis Specification

Competing Model Framing: We confront two mechanistic hypotheses. H_0 adopts a nonlinear Wiener process, capturing intricate degradation patterns through greater model flexibility. H_1 , representing a simpler model with fewer parameters, constrains the path to a linear Wiener process.

Step 2: Probabilistic Foundation

The core inference leverages the likelihood $\ell(\theta|x)$ quantifying data plausibility under parameters θ , where $\theta \in \Psi$. For a multivariate normal distribution, assuming the sample $\mathbf{X} = (\mathbf{X}_1, \mathbf{X}_2, \dots, \mathbf{X}_n)^T$ follows a multivariate normal distribution, this function takes the canonical form:

$$\ell(\mu, \Sigma|\mathbf{X}) = \prod_{i=1}^n \frac{1}{(2\pi)^{p/2} |\Sigma|^{1/2}} \exp\left(-\frac{1}{2} (\mathbf{X}_i - \mu)' \Sigma^{-1} (\mathbf{X}_i - \mu)\right) \quad (16)$$

where p is the dimensionality of the sample data, and $|\Sigma|$ is the determinant of the covariance matrix Σ_n . For computational convenience, the log-likelihood function $\text{In}\ell(\mu, \Sigma | \mathbf{X})$ is typically used, expressed as:

$$\text{In}\ell(\mu, \Sigma | \mathbf{X}) = -\frac{np}{2} \text{In}(2\pi) - \frac{n}{2} \text{In}|\Sigma| - \frac{1}{2} \sum_{i=1}^n (\mathbf{X}_i - \mu)' \Sigma_n^{-1} (\mathbf{X}_i - \mu) \quad (17)$$

Step 3: Calculate the Likelihood Function Values

Consider the following testing problem: $H_0 : \theta \in \Psi_0 \leftrightarrow H_1 : \theta \in \Psi_1$, where Ψ_0, Ψ_1 are non-empty sets. Under the condition that H_0 holds, the parameters $\hat{\theta}$ are set to the values specified by the null hypothesis, and the likelihood function $\ell_0 = \ell(\hat{\theta}_0 | x)$ is calculated. Taking the logarithm yields the log-likelihood function value $\text{In}\ell_0$. The probability density of each sample point is computed using the mvnpdf function in MATLAB, and the log-likelihood value is obtained by summing the logarithms.

Step 4: Estimate Models and Compute Test Statistic

The degradation data are fitted under both the linear and nonlinear models using maximum likelihood estimation, and the corresponding maximum log-likelihood values are obtained. The statistic is:

$$\hat{\lambda}(x) = -2 \text{In}\left(\frac{\ell_0}{\ell_1}\right) = 2(\text{In}\ell_1 - \text{In}\ell_0) \quad (18)$$

From the above equation, it can be seen that the value of $\hat{\lambda}(x)$ does not depend on the parameter $\hat{\theta}$. When $\hat{\lambda}(x)$ is small, $\ell(\hat{\theta}_0 | x)$ is larger than $\ell(\hat{\theta}_1 | x)$, and the rejection region for the test is:

$$Z = \{\hat{\lambda} \leq \lambda_0\} \quad (19)$$

where λ_0 satisfies $P\{\hat{\lambda} \leq \lambda_0 | H_0\} \leq \alpha$.

Step 5: Decision

Given a significance level $\alpha = 0.05$, the critical value $\chi_{1-\alpha}^2$ is obtained accordingly, under H_0 , the decision rule is binary:

Reject H_0 if $\tilde{\lambda} < \chi_{1-\alpha}^2 (DF)$.

Do not reject H_0 otherwise.

This statistical framework completes the identification and validation of our nonlinear Wiener degradation model. With parameters now statistically justified, the model can directly inform condition assessment and maintenance strategies.

5. Model

Based on the nonlinear Wiener degradation model and its parameter estimation results established in the previous sections, this section constructs a practically oriented CBM decision optimization model for engineering applications. By integrating degradation condition information and maintenance cost structure, it aims to provide scientific and economical maintenance decision support for systems with nonlinear degradation characteristics. Moving beyond conventional cost-minimization frameworks (Yao et al., 2020; Zhao et al., 2021), this work conceptualizes CBM decision-making through a dynamic degradation lens. As illustrated in Fig. 2, vibration signal sensors monitor the component's degradation state at regular inspection intervals Δt , providing real-time health status information. Maintenance interventions are then orchestrated by a nuanced two-tiered threshold policy, dynamically calibrated against the system's evolving health condition to optimize lifecycle cost.

(1) At time t_i^- , if the degradation level meets the inspection maintenance criteria, corrective maintenance is performed, and the number of such actions N_i is recorded.

- (2) At time t_2^- if the degradation hits threshold H_{pm} , the associated preventive maintenance count N_p is incremented.
- (3) At time t_2^+ , if the degradation exceeds threshold H_{cm} , an immediate failure replacement is carried out, and the number of failure replacements N_c is recorded.
- (4) At time t_3^+ , if the degradation exceeds H_{pm} again after a previous preventive maintenance, a further preventive action is performed based on the prior maintenance effect, and N_p is incremented accordingly.

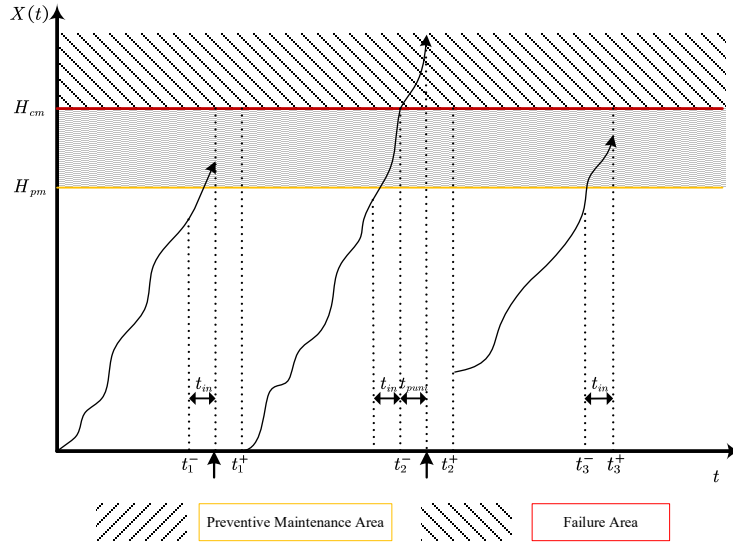


Fig. 2. CBM Strategy Diagram

This model rests on a foundational premise of idealized inspection:

- (1) Inspection processes can accurately condition monitoring capture the true degradation state in real-time.
- (2) The time required for inspection is negligible; the system's health state is captured at discrete inspection points with a fixed interval.
- (3) The initial degradation is zero, and the degradation process is continuous and monotonic. The degradation rate increases with both operating time and the number of prior preventive maintenance actions.
- (4) The duration of all maintenance activities, including minor repair, imperfect maintenance, preventive replacement, and failure replacement, is assumed to be negligible.

This framework strategically balances the inspection interval Δt against the preventive maintenance threshold H_{pm} to maximize lifecycle value. The optimization is driven by an economic criterion minimizing the average cost rate, $E[C(\Delta t, H_{pm})]$, where $C(T)$ aggregates all costs over a single renewal cycle, serving as the pivotal metric. Under a cost-effectiveness criterion, $C(T)$ and $E[C(\Delta t, H_{pm})]$ over the full life cycle v are given by:

$$\min E[C(\Delta t, H_{pm})] = \min \frac{E(C(T))}{E(v)} \tag{20}$$

$$C(T) = N_i \cdot C_{in} + N_p \cdot C_{pm} + N_c \cdot C_{cm} + C_{puni} \cdot T_p(t_d) \tag{21}$$

In the above equation, N_i , N_p , N_c denote the number of inspections, preventive maintenance actions, and corrective replacements up to time t_i , respectively; C_{in} , C_{pm} , C_{cm} are their associated costs; a critical financial penalty is incurred from operational interruptions, quantified as the product of the unit downtime cost C_{puni} and the total duration of downtime $T_p(t_d)$. Therefore, the aggregate cost objective function is constructed as:

$$s.t. \begin{cases} \Delta t > 0 \\ H_{cm} > H_{pm} > 0 \end{cases} \tag{22}$$

$$(\Delta t^*, H_{pm}^*) = \operatorname{argmin} E[C(\Delta t, H_{pm})]$$

6. Case Study

6.1 Case Description

To validate the effectiveness of the proposed nonlinear Wiener process modeling and CBM decision-making methodology, a case study is conducted on a Power Take-Off (PTO) system, a critical component of CNC machine tools. The PTO functions as a complex gear transmission system composed of one or multiple sets of speed-changing gears. It is responsible for distributing power from the main engine to auxiliary devices such as generators and hydraulic pumps. The overall structure and a cross-sectional view of the PTO are illustrated in Fig. 3. As shown, the PTO primarily consists of a gearbox, electric motor, generator, gear transmission mechanism, gear coupling, and electromagnetic clutch. When the chassis engine supplies power, the coupling flange gear transmission mechanism drives the generator and servo pump. Under this condition, the electromagnetic clutch disengages from the transmission part connected to the motor shaft. During operation, wear on components such as gears and bearings is the primary cause of reduced transmission efficiency and increased vibration, which may eventually lead to loss of positioning accuracy or complete failure.

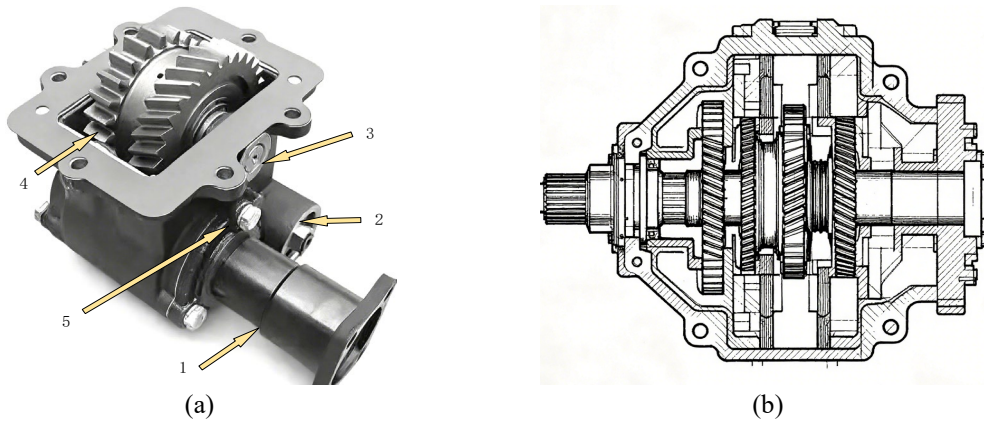


Fig. 3. Overall Structure (a) and Cross-Sectional View (b) of the PTO (1-Generator, 2-Motor, 3-Connecting Flange, 4-Gearbox Magnetic Particle Brake, 5-Plug Screw)

This degradation process exhibits two key characteristics that make it an ideal case for validating the proposed model: First, the degradation trajectory shows a distinct nonlinear acceleration trend, consistent with the basic assumption of time-scale transformation. Second, the stochastic fluctuations observed during the degradation process are well-suited to be characterized by the randomness inherent in the Wiener process. Therefore, the proposed nonlinear Wiener process model can accurately describe its degradation behavior, providing reliable input for subsequent CBM decisions.

6.2 Analysis of Estimation and Testing

Applied to the PTO degradation dataset per Section 4.1, the estimator yielded precise parameter identifications, synthesizing nonlinear least squares with dedicated matrix/vector operations. The calibrated drift coefficient (4.5×10^{-3}) and squared diffusion coefficient (1.4256×10^{-4}) were thus derived. The iterative convergence profile, illustrated in Fig. 4, not only confirms estimation stability but also underscores the algorithmic efficiency and numerical robustness achieved beyond conventional fitting procedures.

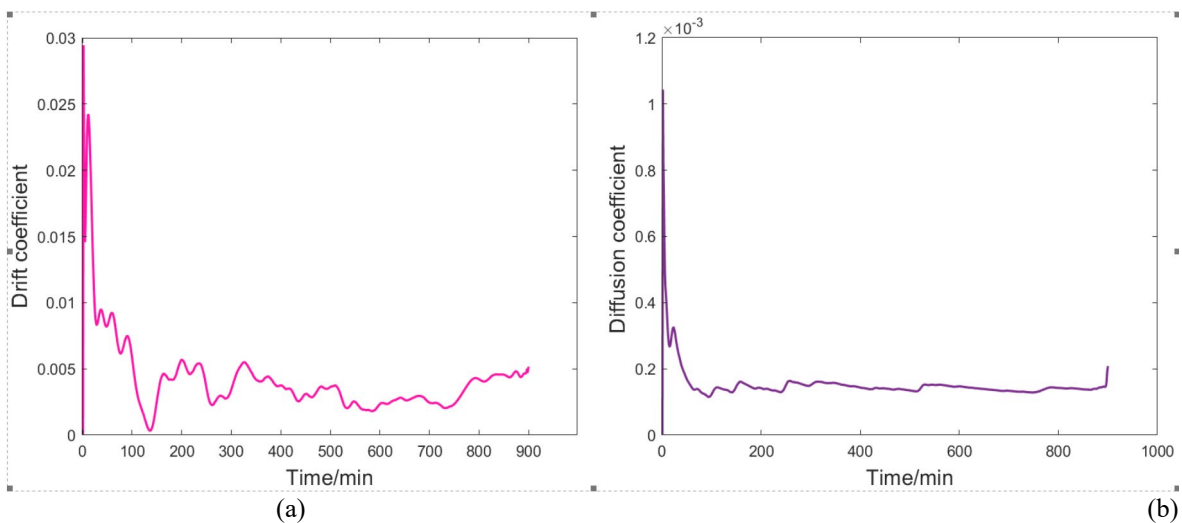


Fig. 4. Iterative Convergence Process

To verify the statistical significance of the parameter estimates, a likelihood ratio hypothesis test was performed as outlined in Section 4.2. The results are as follows:

(1) After conducting 100 simulations of the likelihood ratio statistics for the two coefficients, the results exceeded the critical value only once, yielding an acceptance rate of the null hypothesis of 99.0%.

Contrary to theoretical expectations, the magnitude of the log-likelihood (drift: 4396.6920; diffusion: 4954.5815) under the null hypothesis suggests a more nuanced relationship between the model components and the observed process than is conventionally assumed, compared to 4393.6711 and 4954.5080 under the alternative hypothesis, respectively. These results indicate high credibility of the estimation method as shown in Fig. 5.

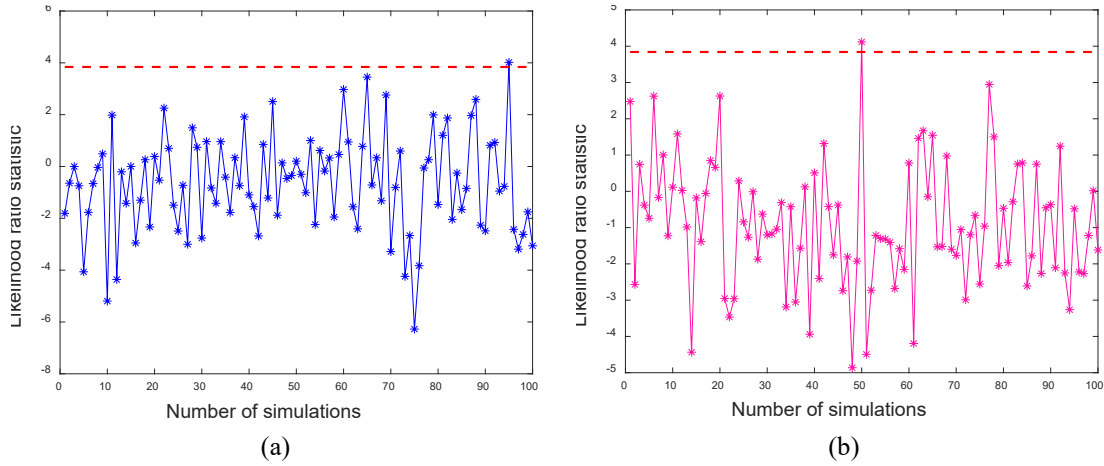


Fig. 5 (a) Drift Coefficient and (b) Diffusion Coefficient Likelihood Ratio Statistics vs. Simulation Iterations

(2) The kernel density plots exhibit sharp peaks for both coefficients, indicating stable and concentrated distributions of the estimated values with low uncertainty, as shown in Fig. 6.

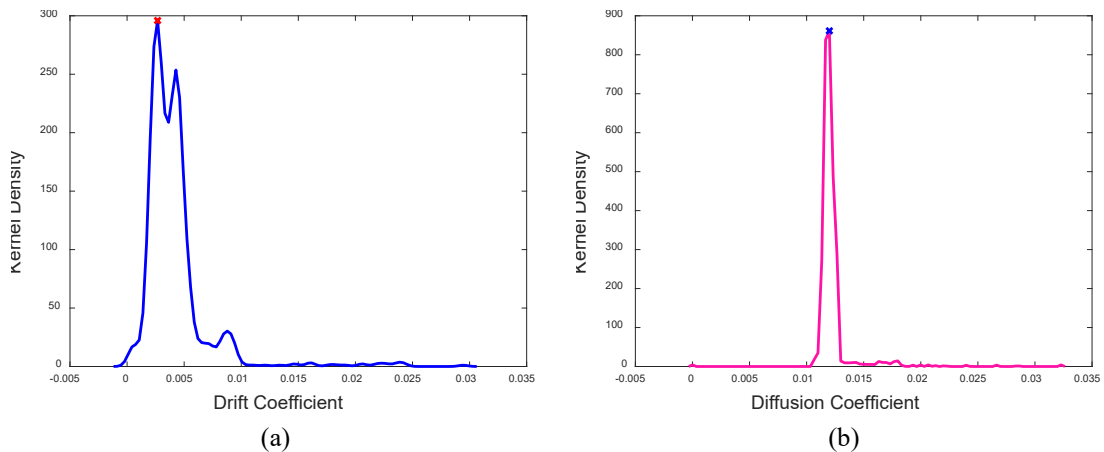
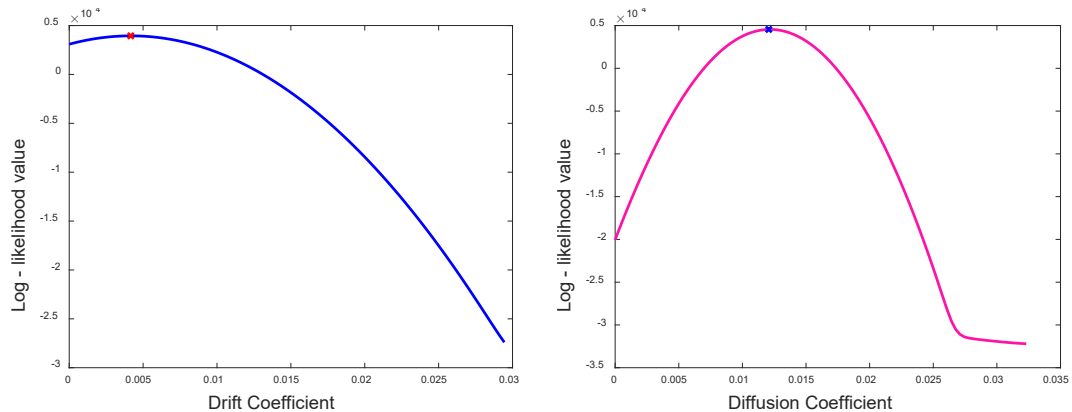


Fig. 6 (a) Drift Coefficient and (b) Diffusion Coefficient Kernel Density Plots

(3) Analysis of the profile likelihood plots reveals that the log-likelihood functions for both parameters are steep, particularly near their peaks. A small change in either parameter leads to a substantial change in the likelihood value, indicating that the parameter estimates are relatively accurate and sensitive to the data fit. The peak values correspond to a drift coefficient of 0.004164 and a diffusion coefficient of 0.012074, as shown in Fig. 7.



(a) (b)
Fig. 7 (a) Drift Coefficient and (b) Diffusion Coefficient Log-Likelihood Plots

(4) The contour plot visualizes the joint confidence region, with color gradients representing varying degrees of deviation. The red dots, representing simulated parameter combinations, cluster primarily in the lower-left quadrant of the confidence region, reflecting consistency and stability in the estimated values, as shown in Fig. 8.

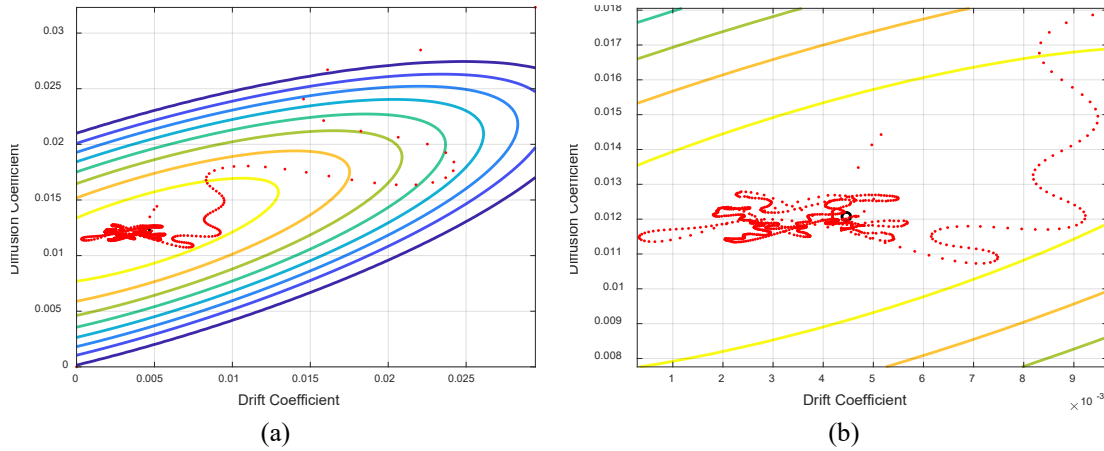


Fig. 8. Joint Confidence Region Plot

In summary, the combined analysis results strongly support the null hypothesis, confirming that the model effectively describes the accuracy, rationality, and reliability of the parameter estimation method.

6.3 Results of Decision Making

Based on the estimated model parameters, the nonlinear degradation trajectory of the PTO system was simulated, as illustrated in Fig. 9. The degradation trajectory of a PTO exhibits a characteristic nonlinear progression. It transitions from a latent accumulation phase, with degradation metrics suppressed below preventive maintenance levels, to a critical failure phase marked by an exponential escalation in deterioration rate, swiftly breaching both preventive and catastrophic failure thresholds.

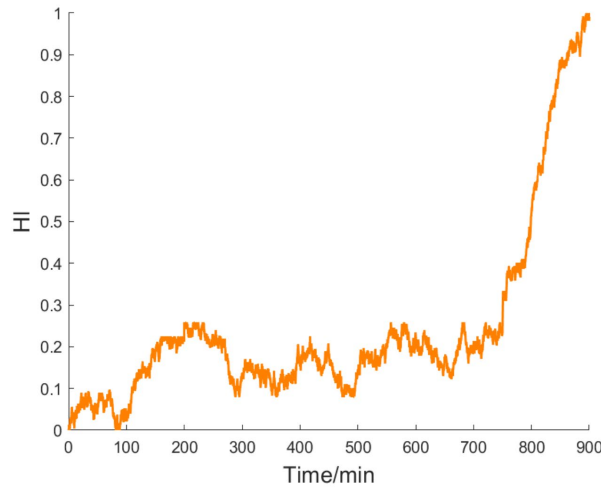


Fig. 9. Degradation Curves Simulated by Nonlinear Wiener Process

To interrogate the cost-effectiveness of the maintenance policy, we systematically varied both the inspection interval Δt and the preventive maintenance threshold H_{pm} across a plausible operational range via Monte Carlo simulation. The analysis converged to a globally optimal configuration of these variables, decisively minimizing the lifecycle maintenance expenditure rate. Given the cost parameters $C_{in}=100$, $C_{pm}=3500$, $C_{cm}=4800$, and $C_{punl}=50$, the minimum value of the objective function was found to be 7.575, with the optimal decision variables Δt and H_{pm} being 59 and 0.66, respectively. Fig. 10(a) and Fig. 10(b) graphically reveal the critical nonlinearities and potential optimization pitfalls in the objective function's response to the two key decision variables.

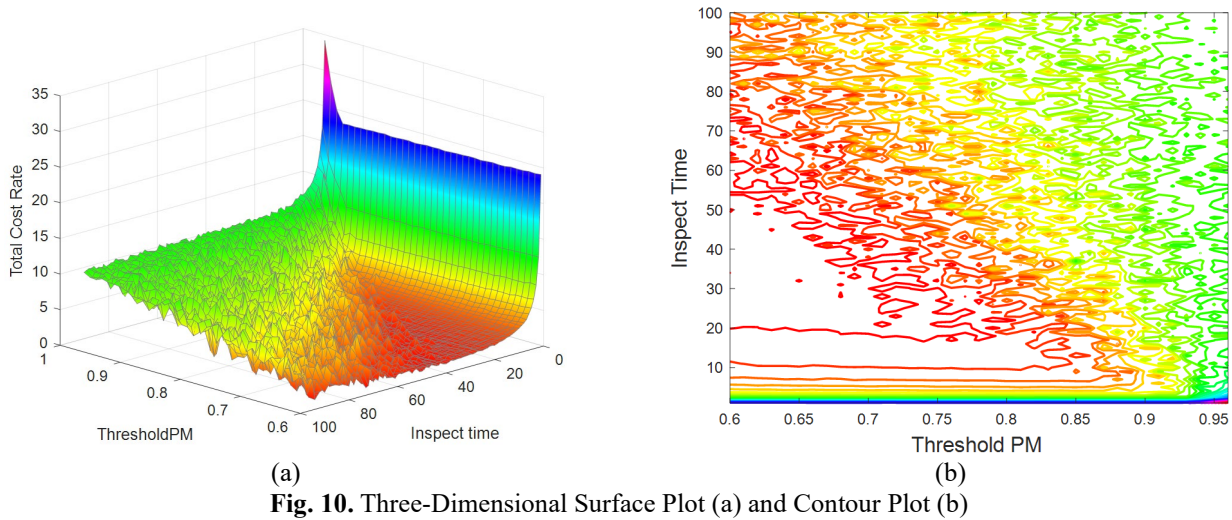


Fig. 10. Three-Dimensional Surface Plot (a) and Contour Plot (b)

As observed in Fig. 10(a) and Fig. 10(b), when Δt is set too short, although system status can be monitored frequently, the associated inspection costs become excessive. Conversely, as Δt increases, the delayed detection of potential failures raises the risk of catastrophic breakdowns, leading to an increase. The derived solution represents a theoretically optimal compromise between maintenance extremes; however, its practical viability hinges on the accurate quantification of often-overlooked failure risks.

A failure in the PTO most directly results in the halt of the gear pump, depriving the hydraulic tipping system of its power source and causing complete operational paralysis. Additionally, the solenoid valve in the control mechanism, due to frequent actuation, is prone to wear and failure, leading to malfunction in gear engagement and disengagement. To address different failure modes, appropriate troubleshooting and repair measures should be implemented. Regular maintenance is essential, including inspection of fastening bolts, monitoring of lubricant condition, and cleaning of components to avoid contamination and physical damage. During the solenoid valve unloading process, regular checks should be conducted on its effectiveness, responsiveness, circuit safety, and switching performance.

6.4 Sensitivity Analysis

In practical maintenance operations, various maintenance costs are closely tied to factors such as spare parts inventory, staffing levels, and labor hours. To evaluate the impact of fluctuations in maintenance cost parameters on the optimal policy, a metric termed the cost rate difference is introduced, calculated as follows:

Given that maintenance cost estimates are often subject to uncertainty, assessing their influence on policy stability is critical. To this end, the cost rate difference Er_i is devised to gauge the vulnerability of the prescribed optimal policy to fluctuations.

$$Er_i = \frac{\widehat{E}_i(C) - E(C)^*}{E(C)^*} \times 100\% \tag{23}$$

This analysis quantifies sensitivity of total maintenance expenditures to $\pm 25\%$ perturbations in each cost parameter relative to established baselines, encompassing inspection, preventive, and corrective actions. The resulting maintenance cost rates and their corresponding Er_i values are summarized in Tables 1–3.

Table 1
Sensitivity Analysis of Inspection Costs

C_{in}	$\Delta C_{in} \%$	$E(C)^*$	Er_i
125	25	8.225	8.581
115	15	7.705	1.716
110	10	7.940	4.818
100	0	7.575	0
90	-10	7.440	-1.782
85	-15	6.925	-8.581
75	-25	6.250	-17.465

Table 2
Sensitivity Analysis of Preventive Maintenance Costs

C_{pm}	$\Delta C_{pm} \%$	$E(C)^*$	E_r
4375	25	8.706	14.931
4025	15	7.829	3.353
3850	10	8.020	5.874
3500	0	7.575	0
3150	-10	7.380	-2.574
2975	-15	6.565	-13.333
2625	-25	6.088	-19.630

Table 3
Sensitivity Analysis of Corrective Maintenance Costs

C_{cm}	$\Delta C_{cm} \%$	$E(C)^*$	E_r
6000	25	7.525	-0.660
5520	15	7.225	-4.620
5280	10	7.600	0.330
4800	0	7.575	0
4320	-10	7.800	2.970
4080	-15	7.300	-3.630
3600	-25	7.050	-6.931

The data demonstrate that the overall cost rate responds with limited sensitivity to C_{in} , despite its approximately linear trend. In stark contrast, C_{pm} governs cost dynamics, particularly imposing severe cost penalties at its upper operational range. This underscores the critical role of resource allocation for preventive maintenance in overall cost control. Changes in C_{cm} have a comparatively minor and more complex effect on the cost rate, which can be attributed to the low probability of costly failure replacements under an effective CBM policy, making long-term average costs less sensitive to fluctuations.

In summary, C_{pm} exhibits the largest variation in E_r among the three cost parameters, highlighting its greater importance in CBM decision-making. These findings offer valuable insights for maintenance managers in budget control and resource planning.

7. Conclusion

Moving beyond linear approximations, we introduce a nonlinear Wiener process with a transformed time scale for CBM. Its embedded power function explicitly models degradation trajectory (slow–stable–fast), a common yet often misrepresented pattern. Model parameters are identified using maximum likelihood estimation and likelihood ratio tests, ensuring statistical reliability. Empirical results demonstrate that our adaptive framework for joint inspection and maintenance planning achieves significant gains over methods reliant on fixed intervals or simplistic linear degradation models. Sensitivity analysis further reveals that the preventive maintenance cost is the most influential factor in the decision-making process, providing clear guidance for practical maintenance resource management.

References

- Alaswad, S., & Xiang, Y. (2017). A review on condition-based maintenance optimization models for stochastically deteriorating system. *Reliability Engineering & System Safety*, 157, 54–63. <https://doi.org/10.1016/j.res.2016.08.009>
- Bai, J., Duan, J., & Han, X. (2024). The likelihood ratio test for structural changes in factor models. *Journal of Econometrics*, 238(2), 105631. <https://doi.org/10.1016/j.jeconom.2023.105631>
- Cai, Y., de Jonge, B., & Teunter, R. H. (2025). Data-driven condition-based maintenance optimization given limited data. *European Journal of Operational Research*, 324(1), 324–334. <https://doi.org/10.1016/j.ejor.2025.01.010>
- Cao, H., Yu, J., & Duan, F. (2025). Condition-based maintenance in complex degradation systems: A review of modeling evolution, multi-component systems, and maintenance strategies. *Machines*, 13(8), 714. <https://doi.org/10.3390/machines13080714>
- Chen, Y., Qiu, Q., & Zhao, X. (2022). Condition-based opportunistic maintenance policies with two-phase inspections for continuous-state systems. *Reliability Engineering & System Safety*, 228, 108767. <https://doi.org/10.1016/j.res.2022.108767>
- Civera, M., & Surace, C. (2022). Non-destructive techniques for the condition and structural health monitoring of wind turbines: A literature review of the last 20 years. *Sensors*, 22(4), 1627–1647. <https://doi.org/10.3390/s22041627>
- de Jonge, B., Teunter, R., & Tinga, T. (2017). The influence of practical factors on the benefits of condition-based maintenance over time-based maintenance. *Reliability Engineering & System Safety*, 158, 21–30. <https://doi.org/10.1016/j.res.2016.10.002>
- Dong, E., Zhang, Y., Zhan, X., Bai, Y., & Cheng, Z. (2024). A novel dynamic predictive maintenance framework for gearboxes utilizing nonlinear Wiener process. *Measurement Science and Technology*, 35(12), 125401. <https://doi.org/10.1088/1361->

6501/ad762e

- Gong, M., Eryilmaz, S., & Xie, M. (2020). Reliability assessment of system under a generalized cumulative shock model. *Proceedings of the Institution of Mechanical Engineers, Part O: Journal of Risk and Reliability*, 234(1), 129–137. <https://doi.org/10.1177/1748006X19864831>
- Hao, S., Chen, W., & Wang, J. (2025). Joint optimization of condition-based operation and maintenance strategy for load-sharing systems subject to hybrid continuous and discrete loads. *Reliability Engineering & System Safety*, 262, 111166. <https://doi.org/10.1016/j.res.2025.111166>
- Li, J., Chen, Y., Cai, Z., & Wang, Z. (2022). A dynamic condition-based maintenance optimization model for mission-oriented system based on inverse Gaussian degradation process. *Journal of Systems Engineering and Electronics*, 33(2), 474–488. <https://doi.org/10.23919/JSEE.2022.000047>
- Lin, F., Wang, L., Li, Z., Yin, L., Wu, J., Zheng, D., Wang, X., & Hu, Y. (2025). Rolling contact fatigue failure mechanism with the multi-scale analysis of BG801 high temperature bearing steel. *International Journal of Fatigue*, 193, Article 108760. <https://doi.org/10.1016/j.ijfatigue.2024.108760>
- Liu, Q., Shen, Y., Sun, Y., Dong, M., & Wang, Y. (2025). Condition-based maintenance optimization for batch production system based on demand fluctuations. *Proceedings of the Institution of Mechanical Engineers, Part B: Journal of Engineering Manufacture. Advance online publication*. <https://doi.org/10.1177/09544054251333648>
- Lu, C. J., & Meeker, W. Q. (1993). Using degradation measures to estimate a time-to-failure distribution. *Technometrics*, 35(2), 161–174. <https://doi.org/10.1080/00401706.1993.10485038>
- Luo, J., Luo, X., Ma, X., Zan, Y., & Bai, X. (2025). An integrated condition-based opportunistic maintenance framework for offshore wind farms. *Reliability Engineering & System Safety*, 256, 110701. <https://doi.org/10.1016/j.res.2024.110701>
- Nguyen, K. A., Do, P., & Grall, A. (2015). Multi-level predictive maintenance for multi-component systems. *Reliability Engineering & System Safety*, 144, 83–94. <https://doi.org/10.1016/j.res.2015.07.017>
- Oakley, J. L., Wilson, K. J., & Philipson, P. (2022). A condition-based maintenance policy for continuously monitored multi-component systems with economic and stochastic dependence. *Reliability Engineering & System Safety*, 222, 108321. <https://doi.org/10.1016/j.res.2022.108321>
- Oh, S. Y., Joung, C., Lee, S., Shim, Y. B., Lee, D., Cho, G. E., et al. (2024). Condition-based maintenance of wind turbine structures: A state-of-the-art review. *Renewable and Sustainable Energy Reviews*, 204, 114799. <https://doi.org/10.1016/j.rser.2024.114799>
- Qiu, Q., Cui, L., & Kong, D. (2019). Availability and maintenance modeling for a two-component system with dependent failures over a finite time horizon. *Proceedings of the Institution of Mechanical Engineers, Part O: Journal of Risk and Reliability*, 233(2), 200–210. <https://doi.org/10.1177/1748006X18768713>
- Sharma, V. B., Singh, K., Gupta, R., Joshi, A., Dubey, R., Gupta, V., Agarwal, S., & Sharma, R. (2021). Review of structural health monitoring techniques in pipeline and wind turbine industries. *Applied System Innovations*, 4(3), 59. <https://doi.org/10.3390/asi4030059>
- Si, X. S., Li, T., Zhang, J., & Lei, Y. (2022). Nonlinear degradation modeling and prognostics: A Box-Cox transformation perspective. *Reliability Engineering & System Safety*, 217, 108120. <https://doi.org/10.1016/j.res.2021.108120>
- Si, X. S., Wang, W. B., Hu, C. H., Zhou, D. H., & Pecht, M. G. (2012). Remaining useful life estimation based on a nonlinear diffusion degradation process. *IEEE Transactions on Reliability*, 61(1), 50–67. <https://doi.org/10.1109/TR.2011.2182221>
- Tan, S., Hu, Q., Guo, C., Zhu, D., Dong, E., Zhang, F., et al. (2025). Operational readiness-oriented condition-based maintenance and spare parts optimization for multi-state systems. *Reliability Engineering & System Safety*, 264, 111367. <https://doi.org/10.1016/j.res.2025.111367>
- Wijnmalen, D. J. D., & Hontelez, J. A. M. (1997). Coordinated condition-based repair strategies for components of a multi-component maintenance system with discounts. *European Journal of Operational Research*, 98(1), 52–63. [https://doi.org/10.1016/0377-2217\(95\)00312-6](https://doi.org/10.1016/0377-2217(95)00312-6)
- Xie, S. L., Xue, F., Zhang, W. M., & Zhu, J. W. (2024). A condition-based maintenance policy for reconfigurable multi-device systems. *Advanced Manufacturing*, 12(2), 252–269. <https://doi.org/10.1007/s40436-023-00465-x>
- Yao, Y. Q. (2020). Reliability modeling and condition-based maintenance strategy for two-stage degradation systems [Doctoral dissertation, Tianjin University]. <https://doi.org/10.27356/d.cnki.gtjdu.2020.001899>
- Ye, Z. S., & Xie, M. (2015). Stochastic modelling and analysis of gradation for highly reliable products. *Applied Stochastic Models in Business and Industry*, 31(1), 16–32. <https://doi.org/10.1002/asmb.2063>
- Zhan, X., Liu, Z., Yan, H., Wu, Z., Guo, C., & Jia, X. (2023). A novel method of health indicator construction and remaining useful life prediction based on deep learning. *Eksploracja i Niezawodność – Maintenance and Reliability*, 25(4), 963–972. <https://doi.org/10.17531/ein/171374>
- Zhang, L., Chen, X., Khatab, A., & An, Y. (2022). Optimizing imperfect preventive maintenance in multi-component repairable systems under δ -dependent competing risks. *Reliability Engineering & System Safety*, 219, Article 108177. <https://doi.org/10.1016/j.res.2021.108177>
- Zhang, Z., Li, H., Li, T., Zhang, J., & Si, X. (2024). An optimal condition-based maintenance policy for nonlinear stochastic degrading systems. *Reliability Engineering & System Safety*, 251, 110349. <https://doi.org/10.1016/j.res.2024.110349>
- Zhao, X. (2021). Research on joint optimization strategy of preventive maintenance for equipment systems based on multi-objective decision making [Doctoral dissertation, University of Science and Technology Beijing]. <https://doi.org/10.26945/d.cnki.gbjku.2021.000403>
- Zheng, H., Yang, J., & Zhao, Y. (2024). Reliability analysis of multi-stage degradation with stage-varying noises based on the

nonlinear Wiener process. *Applied Mathematical Modelling*, 125, 445–467. <https://doi.org/10.1016/j.apm.2023.09.007>
Zhu, B., Dong, E., Cheng, Z., Zhan, X., Jiang, K., & Wang, R. (2026). An integrated approach to condition-based maintenance decision-making of planetary gearboxes: Combining temporal convolutional network auto encoders with Wiener process. *Computers, Materials & Continua*, 86(1), 1–26. <https://doi.org/10.32604/cmc.2025.069194>



© 2026 by the authors; licensee Growing Science, Canada. This is an open access article distributed under the terms and conditions of the Creative Commons Attribution (CC-BY) license (<http://creativecommons.org/licenses/by/4.0/>).